7-28-2020

Investigate the Role of Biofilm and Water Chemistry on Lead Deposition onto and Release from Polyethylene: An Implication for Potable Water Pipes

Tanvir Ahamed

INVESTIGATE THE ROLE OF BIOFILM AND WATER CHEMISTRY ON LEAD DEPOSITION ONTO AND RELEASE FROM POLYETHYLENE: AN IMPLICATION FOR POTABLE WATER PIPES

by

Tanvir Ahamed

A Thesis

Submitted in Partial Fulfillment of the

Requirements for the Degree of

Master of Science

Major: Civil Engineering

The University of Memphis

August 2020

Dedicated to My Family and Advisor

ACKNOWLEDGMENTS

First, I would like to thank my advisor Dr. Maryam Salehi Esfandarani, Assistant Professor in the Department of Civil Engineering at The University of Memphis for her guidance, mentoring, support, patience as well as motivating me through my graduate studies and thesis work.

I am thankful to Dr. Gary Bowlin and Benjamin Minden at the University of Memphis, Biomedical Engineering Department, for their assistance in using the fluorescence microscope and hemocytometer. I also appreciate Dr. Paul Simone and Dr. Gary Emmert at the Chemistry Department for their assistance with the metal's quantifications. Additional thanks to Donya Sharafoddinzadeh in Civil Engineering Department for her help in Atomic Absorption machine utilization. Special thanks to Dr. Felio Perez (Materials Science Lab Manager, The University of Memphis) for assisting in X-ray photoelectron spectroscopy (XPS) analysis.

I would like to express my gratitude toward my parents and my beloved wife for their sacrifices and supports throughout my graduate studies.

ABSTRACT

In this study, the influence of biofilm presence and water chemistry conditions on lead (Pb) deposition onto low density polyethylene (LDPE) surface was examined. The results demonstrated that biofilm presence on LDPE surfaces strongly and significantly enhanced Pb uptake, with 13-fold greater equilibrium Pb surface loading when biofilm was present (1602 $\mu g/m^2$) compared to when it was absent (124 $\mu g/m^2$). Pseudo 2nd order kinetic model best described Pb adsorption to LDPE with biofilm. Pb adsorption onto new LDPE surfaces was significantly reduced from 1101 $\mu g/m^2$ to 134 $\mu g/m^2$ with increased aqueous solution's ionic strength from 3×10^{-6} M to 0.0072 M. The presence of chlorine residual (2 mg/L) significantly reduced Pb adsorption onto LDPE surfaces by possible oxidation of Pb^{2+} to Pb^{4+} species. The kinetics of Pb release from LDPE surfaces was investigated under static and dynamic conditions at pH 5.0 and 7.8.

Keywords*: Lead, Plastic pipes, Biofilm, Adsorption kinetics, Polyethylene*

TABLE OF CONTENTS

LIST OF FIGURES vii

INTRODUCTION 1

EXPERIMENTAL 5

MATERIALS 5

BIOFILM GROWTH AND QUANTIFICATIONS 5

KINETIC EXPERIMENTS: FIVE-DAY Pb EXPOSURE 7

Pb ADSORPTION KINETIC MODELING 8

CHLORINE DECAY EXPERIMENTS 9

Pb RELEASE EXPERIMENTS FROM LDPE SURFACE 10

X-RAY PHOTOELECTRON SPECTROSCOPY (XPS) 10

WATER QUALITY ANALYSIS 11

STATISTICAL ANALYSIS 11

RESULTS AND DISCUSSION 12

INFLUENCE OF BIOFILM ON Pb UPTAKE BY NEW LDPE 12

BIOFILM QUANTIFICATION 12

THE INFLUENCE OF BIOFILM ON Pb DEPOSITION ONTO LDPE 13

INFLUENCE OF WATER CHEMISTRY ON Pb DEPOSITION ONTO NEW AND AGED LDPE 16

Pb SPECIATION IN SYNTHETIC AND DI WATER 16

EFFECT OF ION'S COMPETITION ON Pb^{2+} DEPOSITION ONTO NEW AND AGED LDPE 17

THE INFLUENCE OF CHLORINE RESIDUALS ON Pb DEPOSITION ONTO THE LDPE SURFACE 18

THE INFLUENCE OF CHLORINE RESIDUALS ON THE KINETICS OF Pb DEPOSITION ONTO NEW LDPE 18

OXIDATION OF LDPE SURFACE ACCUMULATED Pb^{2+} TO Pb^{4+} 20

INVESTIGATE THE FACTORS INFLUENCE Pb RELEASE FROM LDPE SURFACE 21

IMPLICATION TO THE POTABLE WATER PLUMBING PIPES 24

CONCLUSION 26

REFERENCES 27

SUPPLEMENTAL INFORMATION 34

LIST OF FIGURES

Figure 1: Binary images showing biofilm-covered regions on the LDPE film surface..... 13

Figure 2: The experimental results (Mean $\pm$ std) and Pseudo 2nd order model for Pb surface loading ($\mu g/m^2$) on LDPE/no biofilm and LDPE/biofilm overtime at pH 7.8 15

Figure 3: Log concentrations for Pb^{2+} species versus the water pH, $[Pb]_t$ = 300 µg/L..... 16

Figure 4: Pb surface loading on (A) new LDPE and (B) aged LDPE in DI water and synthetic water at pH 7.8..... 18

Figure 5: Pb surface loading on LDPE with presence and absence of chlorine residuals 20

Figure 6: X-ray photoelectron spectroscopy (XPS) spectra of Pb..... 21

Figure 7: Percentage of Pb release from new LDPE at pH 5.0 and 7.8 (dynamic condition) (Left) 23

Figure 8: Percentage of Pb release from new and aged LDPE surface at pH 5.0 (dynamic condition) (Right)..... 23

INTRODUCTION

Lead (Pb) exposure through municipal tap water is a critical health concern nationally and globally. Lead in tap water remains an ongoing serious threat to public health, with recent large scale lead exposures occurring in Washington (DC), Flint (MI), and Newark (NJ) in the United States.[1,2,3] While the U.S. Environmental Protection Agency (US EPA) lead action level in drinking water is 15 µg/L, it was recommended by the American Association of Pediatrics that children do not expose to lead in drinking water at levels above 1 ug/L. The American Academy of Pediatrics recommended that children should not be exposed to lead in drinking water at levels greater than 1.0 µg/L. Lead exposure can result in severe acute and chronic health impacts such as irreversible developmental and behavioral delays in children, hearing problems, renal dysfunction and delay in postnatal growth.[4,3,5,6] Lead in tap water predominantly originates from corrosion of lead-bearing plumbing materials including lead service lines, brass valves and fittings, galvanized iron, lead-tin solder, and faucets.[7,8] The recent field investigation revealed the Pb release (1-13 µg/L) to the residential building tap water however, the building plumbing was plastic (PEX-a) and the service line was Copper.[9] These low levels of Pb in residential plumbing in the absence of lead component piping showed variable levels across plumbing fixtures. Lead likely originated from ball valves, brass barb tees, brass elbows, and faucets in this system.[10,11] Elfland et al., (2010) reported lead levels as high as 350 µg/L from the water fountains in a new building which the brass fittings were contributed to this lead contamination.[12]

The goal of increased sustainability coupled with the lower installation costs of plastic pipes has driven the increased usage for building plumbing renovations and construction of new potable water systems. The global demand for plastic pipes has been estimated to be growing

more than 4% per annum.[13] Plastic pipes are considered durable and easy to install, which further stimulates the demand. Moreover, the smooth plastic pipe surfaces are considered to be less susceptible to the accumulation of deposits.[14,15] Additionally, polymer plastic pipes do not have corrosion problems like their metallic and concrete counterparts.[16] Building owners can receive LEED certification by the U.S. Green Building Council if they install plastic instead of copper piping.[17] Crosslinked polyethylene (PEX) pipes are being installed in 75% of new building construction and 54% of renovations in the U.S., and high density polyethylene (HDPE) is used for water service connections.[18] Lead service lines, which are frequently found in the older buildings, are often connected to the recently renovated building plastic plumbing system. Thus, service line corrosion products can be released into the building plumbing and subsequently accumulate on the plastic pipes' inner walls. Our recent studies have demonstrated plastic plumbing pipes can play a major role in heavy metal accumulation by providing micro-resting sites where the presence of surface oxidized functional groups including >C-O<, >C=O, >COO can promote Pb species accumulation onto the low density polyethylene (LDPE) surface.[4,19,11] There has been extensive research conducted on plastic pollution within marine and fresh water environment has demonstrated the influence of water chemistry conditions such as pH, ionic strength, ions competitions that directly influences metal adsorption onto the plastics.[20,21,22] However, mechanistic understanding of how these parameters influence heavy metals accumulation onto the plastic drinking water plumbing is still lacking. Plastics are generally considered chemically inert materials with no inherent surface charge, but long term exposure to disinfectant residuals, surface precipitation of minerals scale, and biofilm accumulation could increase their susceptibility as a charged and porous media for heavy metals adsorption.[20] Further, plastic aging influences Pb uptake by LDPE pellets by forming and increasing the

diversity of polar functional groups on the LDPE surface and by altering LDPE surface morphology.[19] The recent study has shown that 10 h ozone aged LDPE pellets adsorbed up to 5 times more of heavy metals (Cu, Mn, Pb, and Zn) than new LDPE pellets.[11] A significant reduction was found in the Pb surface loadings on new and aged LDPE pellets when water pH is increased from 7.8−11 at a Pb concentration of 300 μg/L.[19] Water chemistry fluctuations could result in detachment and dissolution of Pb corrosion products into tap water.[23,24,25] The effect of disinfectant residuals on heavy metal release from metallic drinking water distribution pipes has been well studied [26–28], but their influence on heavy metal fate in plastic plumbing materials has received much less scrutiny. Free chlorine residuals present in distribution systems could rapidly oxidize Pb^0 to Pb^{2+} and subsequently to Pb^{4+}, which can aid in the precipitation of Pb in the form of α-PbO_2 (scrutinyite) and β-PbO_2 (plattnerite) as shown by Eq 1 and 2.[29]

$$Pb + HOCl + H^+ \rightarrow Pb^{2+} + Cl^- + H_2O \qquad E_H^0 = 1.47\ (V) \qquad (1)$$

$$HOCl + Pb^{2+} + H_2O \rightarrow PbO_2 + Cl^- + 3H^+ \qquad E_H^0 = 1.48\ (V) \qquad (2)$$

Microorganisms ubiquitously present in municipal water sources can colonize on the pipe surfaces and many of these can produce extracellular polymeric substances (EPS) which facilitates additional microbial adherence until it creates a biofilm that continues to grow and can even propagate thereby establishing new biofims.[30] Biofilms may adhere to the pipe surface initially by the weak van der Waals forces and hydrophobic effects. These biofilms can accumulate on pipe surfaces and critically influence the heavy metal fate and transport within the plastic plumbing.[32] Biofilms present on plastic surfaces improve heavy metal adsorption capacity by altering the surface charge, surface roughness, surface free energy, and electrostatic interactions.[33,34] Marine plastic pollution studies have confirmed the role of biofilms in increased heavy metal uptake by microplastics.[35] However, there is a knowledge gap in how biofilms

influence contaminant fate in plastic plumbing materials. While research has been conducted on the interactive effects of biofilms on pipe corrosion, [36,37,38] the mechanistic role of biofilms on heavy metal uptake by plastic pipes has been overlooked. Metal deposition onto plastic pipes is not necessarily a public health threat by itself but can become so when these deposited metals are released into the water. Heavy metals deposited onto the pipe surface could release to the water under certain chemical, water flow or microbiological conditions. The fluctuations of water chemistry from using blending or differently sourced water can result in heavy metal dissolution from scales into water. Heavy metals could be released from water distribution networks and plumbing materials into water due to chemical or biological oxidations or physical mechanisms (hydraulic turbulence).[39,40,41] With increased demand and installation of plastic piping materials for potable water systems, additional research is essential to understand the drivers of heavy metals fate and transfer within these materials.

This research aims to examine the factors that influence Pb^{2+} deposition onto and release from LDPE surface biofilms. The LDPE polymer in the form of pellets and films were used for this study as the model plastic due to its simple chemical structure to facilitate surface characterization, biofilm quantifications, and exclude the influence of plastic additives incorporated into the pipe chemical matrix. It is important to note that LDPE pipes are not used for drinking water piping in the U.S., but are used in Europe for different domestic and irrigation purposes.[19] The specific objectives were to (1) investigate the impact of biofilms on Pb deposition onto LDPE; (2) examine the impacts of water chemistry conditions on Pb deposition onto LDPE, and (3) determine the factors that influence Pb release from LDPE surfaces.

EXPERIMENTAL

MATERIALS

Low density polyethylene (LDPE) pellets were purchased from Sigma Aldrich (St. Louis, MO, USA). These pellets had an average diameter of 4.2 mm, and an average mass of 26 mg. The Lead (Pb) ICP-MS standard (1000 mg/L) and sodium hypochlorite (NaOCl) were purchased from RICCA (Arlington, TX, USA) and Alfa Aesar Chemical Inc (Tewksbury, MA, USA) respectively. LDPE plastic films were purchased from McMaster-Carr (Santa Fe Springs, CA, USA) and were cut into the square shape (0.5 cm ×0.5 cm) prior to experiments. Ultrapure Milli-Q™ (18MΩ*cm) treated water was used to conduct all the experiments in this study. In addition to the new LDPE pellets, LDPE pellets aged according to the method described by Salehi et al. (2018) by purging ozone for 10 h were utilized for X-ray Photoelectron Spectroscopy (XPS) study and 7.5 h aged LDPE pellets were utilized for Pb release experiments.[19] The phosphate-buffered saline (PBS) buffer solution (10X) was purchased from Thermo Fisher Scientific Inc (Waltham, MA, USA). Rhodamine 6G stain (excited at 504 nm) was bought from EMD Chemical Inc (Gibbstown, NJ, USA). The synthetic tap water is used for all metal exposure and release experiments. Its composition was adapted from literature [11] and is shown in **Table SI-1**. More details regarding the materials used in this study are described in **SI-1**.

BIOFILM GROWTH AND QUANTIFICATIONS

In this study, initially, the biofilms were grown onto the new LDPE pellets for 32 days at 22 ºC (± 2 ºC) using municipal tap water. For this purpose, LDPE pellets were placed in a glass flask connected to a drinking water fixture located in the Environmental lab. The water was drained from the outlet of the flask where it was covered by the plastic net to prevent the LDPE pellets from leaving the system (**Figure SI-1**). The municipal tap water is taken from

groundwater sources and treated with aeration, chlorination, and fluoridation by the local water utility before delivery. The chemical characteristics of finished water as reported by the local water utility are listed in **Table SI-2**. Following the literature, to grow the biofilm onto the pellets, a methodology whereby pellets are subjected to a water flow of (0.35 L/min) for 12 h and stagnation for 12 h was selected.[42] An automated controlled solenoid valve was installed to open and close the valve to provide the designated water flow and stagnation periods. During the biofilm growth process, total chlorine residual, pH, and temperature were monitored weekly. The average total chlorine and water pHs were 1.1 mg/L (± 0.05) and 7.3 (± 0.10), respectively.

For visualization and quantification purposes, an additional process of growing the biofilm onto LDPE film (0.5 cm × 0.5 cm squares) was conducted. In this process, LDPE films that had undergone the biofilm growth process for 15, 30, 45, 60 and 90 days were removed from the flask. To quantify the surface area covered by biofilm the films were stained with 5 µL of rhodamine 6G for 3 min and rinsed with a PBS buffer solution. [43,44] Because rhodamine 6G binds strongly to negatively charged nucleic acids and proteins that are major components of biofilms, this allows fine-scale fluorescent imaging of biofilms.[45] Images were taken on nine squares (16 mm × 16 mm) for each film using Olympus BX43F (100 W Mercury Lamp Fluorescence Illuminator, 10X–40X magnification, 400–525 nm wavelength) equipped with an Olympus DP73 high-performance digital color camera and fluorescent light source. Images were taken by following a line from the center to the outer edge of each film. Image processing was implemented using MATLAB programming (Matlab™ vers. 9.4, The Mathworks, Inc) to obtain the binary images and calculate the percentage of area covered by biofilm.

To quantify biofilm accumulated onto the LDPE film surfaces, ten LDPE square films were placed in a 15 mL centrifuge tube containing 3 mL of PBS buffer solution (2X) on a shaker (250

rpm, 15 min) to remove loosely adherent cells from the plastic surface. After that, the films were subjected to sonication using a sonication probe (output frequency 20 kHz, power 50 W, volts 24V DC, current 3.75A max) for 5 min. The plastic tubes containing the films were cooled (4 ºC) during sonication steps to prevent heat damage to the microbial cells. The PBS solutions were centrifuged (Eppendorf MiniSpin Plus 5453) at 4000 rpm for 5 min. Then, 5 µL of rhodamine 6G stain was added to the sample and stained for 5 min. After that, 10 µL of each sample was pipetted onto a hemocytometer (Hausser Scientific Bright-Line™) and quantified using a rhodamine light cube. Respective cell numbers were calculated to present as cell densities per unit surface area of films (cells per cm^2). Three replicates were examined at each period, according to the method mentioned. Control experiments were conducted by taking the images of the stained film surface before and after the biofilm separation process to validate the effectiveness of the biofilm separation method (**SI-3**).

KINETIC EXPERIMENTS: FIVE-DAY Pb EXPOSURE

New and aged LDPE pellets were conditioned following Salehi et al., 2018 [19] to exclude the influence of residual organics **(SI-2)**. The five-day Pb exposure experiments were conducted at pH 7.8 for new and aged LDPE pellets and pellets with biofilm. In these experiments, synthetic tap water was used. The surface area to volume ratio for the pellets was selected as 0.85 cm^2/mL similar to Salehi et al., 2018.[19] The Pb uptake by LDPE pellets was investigated after 2, 6, 12, 24, 48 h, and five days of exposure to the aqueous Pb solution ($[Pb]_t$=300 µg/L). Although a wide range of Pb concentration in potable water was reported in the literature (15 µg/L to 18,800 µg/L),[6] but those extreme cases may rarely occur, so in this study a value which is 20 times greater than USEPA action level (15 µg/L) is selected. Furthermore, selecting this Pb concentration enabled the authors to compare their results with recent relevant published

works.[19,46] During the experiments, three replicates (50 mL PTFE bottles) were removed at each time interval. To quantify Pb adsorbed by LDPE, the pellets were removed from the water and acidified with 2% HNO_3 for 24 hr.[4,19,46,47,48] Control experiments were conducted to quantify Pb on LDPE pellets that were colonized by biofilms but were not exposed to metal (Pb) solution. The influence of total chlorine residual on Pb deposition onto LDPE pellets was investigated by adjusting an initial total chlorine concentration of 2.0 ± 0.1 mg/L in an aqueous Pb solution of 300 µg/L and conducting the described kinetic experiment at pH 7.8.

Pb ADSORPTION KINETIC MODELING

The kinetics of Pb^{2+} uptake by LDPE pellets was studied using the Pseudo 1st order and 2nd order kinetic models. The Pb^{2+} uptake by new LDPE pellets was considered as a mass transfer process, as the Pb^{2+} species only transferred from the bulk solution to the plastic surface and no chemical reactions occurred. The Pseudo 1st order rate constant was determined using Eqs (3-5): [49,50]

$$\frac{dq}{dt} = -K_1(q - q_{eq}) \quad (3)$$

$$q = q_{eq}(1 - e^{-K_1 t}) \quad (4)$$

$$t_{\frac{1}{2}} = \frac{ln2}{K_1} \quad (5)$$

Where q is the amount of Pb surface loading on LDPE (µg/m^2) at any given time t (hr), q_{eq} is the amount of Pb surface loading on LDPE (µg/m^2) at equilibrium. The slope of the straight-line plot of ln(q_{eq}-q) against t was used to calculate the Pseudo 1st order reaction rate constant for adsorption K_1 (h^{-1}). The q_{eq} is approximated by taking the average of the last two concentrations in the exposure periods. The half-life (t ½) represents the time required for a polymer to uptake half of equilibrium Pb surface loading and calculated using Eq 5.

The Pseudo 2nd order kinetic model (Eq 6-8) is generally applied when chemical reactions or association controls the adsorption process.[51] Where q is the amount of Pb surface loading on LDPE (µg/m^2) at any given time t (hr), q_{eq} is the amount of Pb surface loading on LDPE (µg/m^2) at equilibrium and h, is the initial adsorption rate at t→0. The Pseudo 2nd order reaction rate constant, K_2 and q_{eq} values can be determined from the slope and intercept of the straight-line plot of t/q versus t. Both adsorption rate constants K_1 and K_2 are the time scaling factor, the value of which describes how fast the system reaches the equilibria. In this study, the distribution ratio (D) shows the Pb distribution between the LDPE surface and aqueous solution. The equation for the distribution ratio is shown in Eq 9.

$$\frac{dq}{dt} = K_2(q_{eq} - q)^2 \quad (6)$$

$$\frac{\mathrm{t}}{q} = \frac{1}{h} + \frac{t}{q_{eq}} \quad (7)$$

$$h = \mathrm{K}_2 q_{eq}^2 \quad (8)$$

$$D(mm) = \frac{Pb\ Surface\ loading\ (\frac{\mu g}{m^2})}{Pb\ floc\ left\ in\ solution(\frac{\mu g}{L})} \quad (9)$$

CHLORINE DECAY EXPERIMENTS

The kinetics of chlorine decay in an aqueous solution containing new LDPE pellets was examined in the presence and absence of Pb^{2+} species ($[Pb]_t$=300 µg/L) through five days of exposure. The experiments were conducted at room temperature at pH 7.8, with an initial total chlorine concentration of 2.0 ± 0.1 mg/L. Total chlorine concentration was measured after 2, 6, 12, 24, 48 h, and five days of exposure periods. All the experimental total chlorine concentrations data were fitted into the 1st order chlorine decay model.[52]

Pb RELEASE EXPERIMENTS FROM LDPE SURFACE

Before conducting the Pb release experiments, both new and aged LDPE pellets were exposed to a Pb^{2+} solution ($[Pb]_t$=300 µg/L) for five days at pH 7.8. Pellets, which were aged for 7.5 h according to the method described by Salehi et al., 2018, [19] were used for release investigations. Twenty pellets were placed in 13 mL of solution in PTFE bottles to have a surface to volume ratio of 0.85 cm^2/mL. The Pb concentrations in aqueous solution and their loadings onto the plastic pellets were analyzed for three replicates at each time interval. After five days of Pb accumulation, the pellets were immediately exposed to the synthetic water at pH 5.0 under both stagnant and dynamic conditions, and at pH 7.8 under dynamic condition. Then the Pb release from pellets into the synthetic water was investigated by quantification of Pb in the contact water after 5 min, 2, 6, 12, 24, 48 h and five-day exposure periods. Furthermore, to quantify the Pb left on the pellets, they were removed from the aqueous solution and acidified with 2% HNO_3 for 24 h.

X-RAY PHOTOELECTRON SPECTROSCOPY (XPS)

The X-ray photoelectron spectroscopy (XPS) was conducted to examine Pb oxidation due to the exposure to chlorine residuals. The 10 h ozone aged LDPE films were used for this XPS analysis to enhance the Pb accumulation onto the LDPE surface and improve its detection by XPS spectroscopy.[19] These aged LDPE films were exposed $[Pb]_t$=10 mg/L and total chlorine concentrations 10 mg/L at pH 7.8, for 48 h and room temperature. The reason for increasing the Pb concentration at this experiment is related to the limitations involved in the X-ray photo electron spectroscopy (XPS). The preliminary tests revealed difficulties in identification the Pb oxidation states even at the Pb concentration of 5000 µg/L. The XPS spectroscopy was performed using a Thermo Scientific spectrometer XPS equipped with a monochromatic Al Kα

radiation ($h\upsilon$ = 1486.6 eV). More details are described in **SI-4**.

WATER QUALITY ANALYSIS

Water pH was measured using a Fisherbrand™ accumet™ XL600 pH Meter. Pocket Colorimeter™ II, Chlorine was used to measure the total chlorine residual (detection limit 0.01 mg/L). Total Pb concentration in water was quantified using the Atomic Absorption spectrometer (AA400, HGA 900 Graphite Furnace). The instrument was calibrated using seven standards (0 μg/L, 5 μg/L, 50 μg/L, 100 μg/L, 150 μg/L, 200 μg/L, 300 μg/L). The limit of detection (LOD) was 2 μg/L (AAS). All standard curves had a coefficient of determination in the range of 0.95 to 0.99.

STATISTICAL ANALYSIS

SPSS 26 was used to perform statistical analysis. The correlation between Pb uptake by LDPE pellets with a total chlorine residual was investigated by Pearson correlation at a 95 % confidence interval. Multiple regression models and student t-tests were performed to identify the significant difference of Pb surface loading of different experiments. Statistical significance was assumed when adjusted p-value < 0.05.

RESULTS AND DISCUSSION

INFLUENCE OF BIOFILM ON Pb UPTAKE BY NEW LDPE

BIOFILM QUANTIFICATION

The fluorescence microscopy imaging of the stained LDPE films revealed increased biofilm surface coverage over time, as shown in **Figure 1**. The percentage of the surface area covered by biofilms has been calculated by dividing the number of white pixels to the total number of pixels for each binary image.[53,54,55] As **Figure SI-2** demonstrates the percentage of the plastic surface area covered by biofilm increased exponentially (*Adj.* $R^2 = 0.93$, $p < 0.05$) from 5.5 % after 15 days to 54 % after 90 days biofilm growth process. The solid-liquid interface between the film surface and aqueous medium may provide a proper environment for the further attachment and evolution of microorganisms. The initial microorganisms that bind can change LDPE surface properties so that additional cells can adhere via cell-to-cell association which may increase the stability of the biofilm community.[30,34] Using the biofilm separation and quantification processes described in **section 2.2** the number of cells per unit area of LDPE films was estimated as 76 ± 15 cells/cm^2 after 15 days of the biofilm growth process which was increased to 650 ± 55 cell/cm^2 after 90 days ($T = 8.16$, $F = 66.64$, *Adj.* $R^2 = 0.96$, $p = 0.004$). As shown in **Figure SI-3**, the average number of cells per unit surface area of LDPE films follows an incremental order.

To validate the efficiency of the biofilm separation process, the described image analysis approach was conducted for fluorescent images captured from five different stained LDPE films before and after the biofilm separation process (**SI-3)**. The results revealed that on average, 70 % ± 6 % biofilm surface coverage was separated (**Figure SI-4**). Both approaches were applied to quantify the biofilm surface loadings onto the LDPE films confirmed the increased biofilm growth over time.

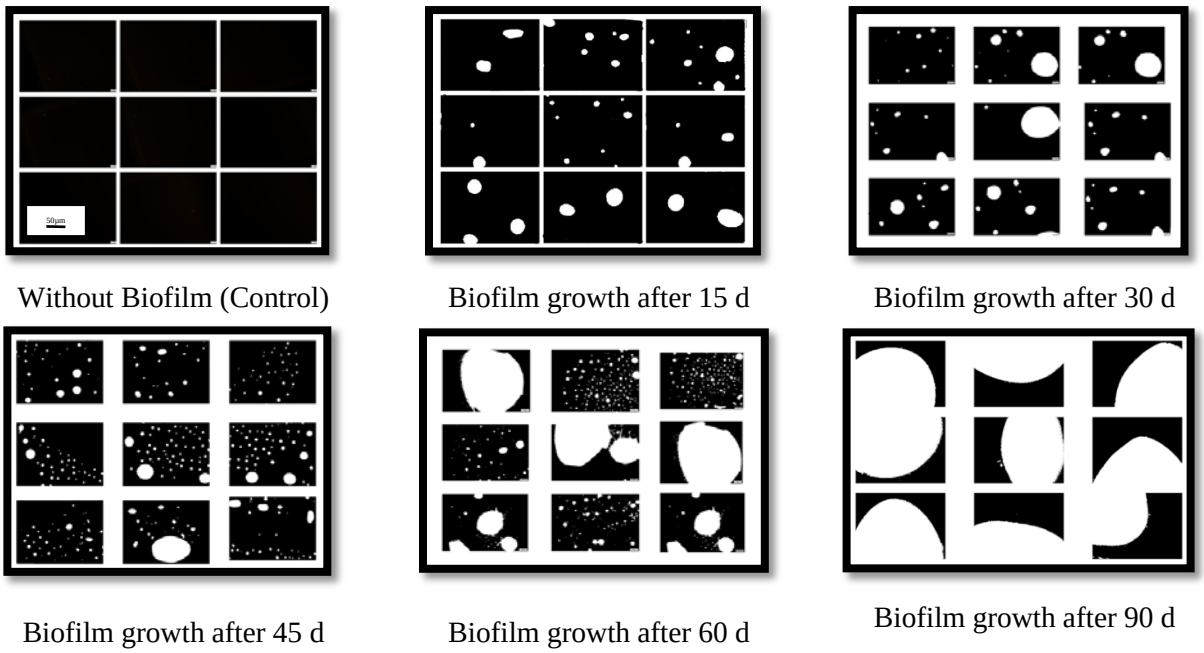

Figure 1*: Binary images showing biofilm-covered regions on the LDPE film surface*

THE INFLUENCE OF BIOFILM ON Pb DEPOSITION ONTO LDPE

The biofilms developed after 32 days onto the new LDPE pellets strongly and significantly (*Tstat = -12.08, Tcrit = 2.77, p = 0.0003*) enhanced the Pb^{2+} adsorption during the 5-day exposure period (**Figure 2**). At equilibrium, the Pb surface loading on LDPE pellets with the biofilm (1602 µg/m^2) was more than 13-fold greater than the new LDPE with no biofilm (124 µg/m^2). While the LDPE surface with biofilm achieved 62.5 % of its surface loading equilibrium during the first 2 h exposure, the LDPE with no biofilm obtained only 36 %. The Pb adsorption onto LDPE with biofilm increased during the 5-day exposure period, however for the LDPE with no biofilm, Pb surface loading reached equilibrium within 6 hr. The distribution ratio (D) of 16.6 and 0.5 for LDPE with biofilm and no biofilm, respectively demonstrated the higher affinity of Pb^{2+} species toward the plastic surface covered by biofilm compared to the condition where biofilm was absent. The biofilm accumulation onto LDPE promoted the availability of surface sites for Pb deposition.[56] Microbial cell walls contain numerous anionic functional

groups (−COOH and $-PO_3^{2-}$), which may facilitate the adsorption of Pb^{2+} complexes onto the cell surface.[57] The extracellular polymeric substances (EPS) are a major component of biofilms are composed of several natural polymers (polysaccharides, proteins, lipids, and nucleic acids) with negatively charged functional groups like hydroxyl (OH^-) and sulfate (SO_4^{2-}) which may also enhance the electrostatic attraction of Pb^{2+} species toward the plastic surface. Other cellular processes like bioaccumulation,[58] biotransformation, and passive processes like adsorption onto microbial cells, may also impact the Pb^{2+} uptake.[59]

The experimental and calculated q_{eq} values, Pseudo 1st order and 2nd order rate constants, half-life (t ½), distribution ratio (D), and coefficient of determinations (R^2) are summarized in **Table 1**. Using the Pseudo 1st order kinetic model, the equilibrium rate constants were determined as 0.0152 (h^{-1}) and 0.0388 (h^{-1}) for LDPE with biofilm and no biofilm, respectively. Thus, LDPE with no biofilm attained the equilibrium surface loading in a shorter time than LDPE with biofilm. These results indicate that the adsorption of Pb^{2+} onto the LDPE with biofilm follows the Pseudo 2nd order kinetic model, as the chemical association was the potential rate-controlling factor. This finding agrees with the other studies which reported the Pseudo 2nd order kinetic model for biosorption of Pb^{2+} ion from aqueous solution by biofilm biomass; however no one investigated Pb^{2+} adsorption onto plastics surface in presence of microbial cells.[60,61,62]

Table 1: *The parameters for Pseudo 1st order and 2nd order kinetics models*

LDPE	Pseudo 1st order model			Pseudo 2nd order model				Distribution Ratio (mm)
	K (h^{-1})	R^2	$t_{½}$ (h)	$q_{eq,}$ Exp ($\mu g/m^2$)	K ($m^2\mu g^{-1}h^{-1}$)	R^2	$q_{eq,}$ Cal ($\mu g/m^2$)	
No Biofilm	0.0152	0.89	45.40	124	0.0016	0.97	119	0.50
With Biofilm	0.0388	0.99	17.80	1602	0.0001	0.99	1667	16.65

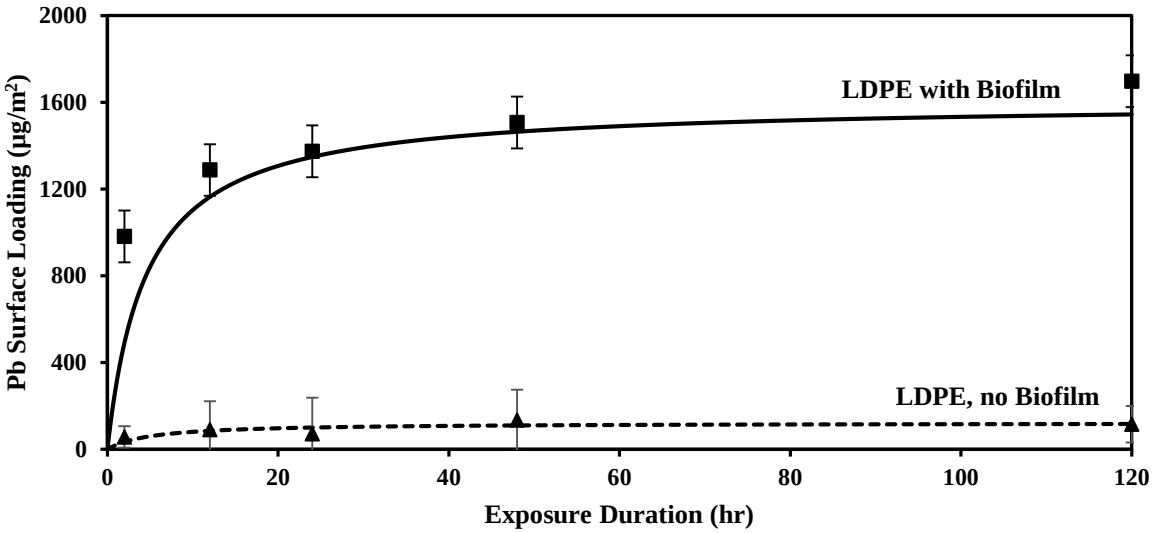

Figure 2*: The experimental results (Mean* $\pm$ *std) and Pseudo 2nd order model for Pb surface loading (µg/m²) on LDPE/no biofilm and LDPE/biofilm overtime at pH 7.8*

Following an increased LDPE film surface coverage by the biofilm, it was expected to have an increased order of Pb uptake by these films. Despite this expectation, conducting the 48 h Pb^{2+} adsorption experiments using the LDPE films that undergone the biofilm growth process for 15 d, 30 d, 45 d, 60 d and 90 days have not revealed an ascending Pb surface loading order (**Figure SI-5**). The reason behind this may be the removal of individual cells or small groups of cells from the surface of the biofilm as the result of shear forces exerted by mixing the solution during the metal exposure experiment. This can also suggest that the LDPE films adsorbed Pb^{2+}

and with biofilm growth, this surface adhered Pb was removed by the bacteria for bio-sequestration, therefore; when cells were removed, this Pb consequently went to the solution.

INFLUENCE OF WATER CHEMISTRY ON Pb DEPOSITION ONTO NEW AND AGED LDPE

Pb SPECIATION IN SYNTHETIC AND DI WATER

As **Figure 3** demonstrates Pb^{2+} ions form a variety of complexes with several anions (OH^-, $SO_4^{2-}, NO_3^-, Cl^-, HPO_4^{2-}, HCO_3^-, SiO_3^{2-}$) present in the synthetic drinking water. In this system, both $Pb(OH)_2$ and $PbCO_3$ were precipitated. However, they only create the hydroxyl complexes ($Pb(OH)^+$, $Pb(OH)_{2\ (aq)}$, $Pb(OH)_2$ (s), $Pb(OH)_3^-$ and $Pb(OH)_4^{2-}$) in the DI water.[19] The Pb^{2+} speciation in synthetic water was determined through solving Pb^{2+} complexation and solubility equations (**Table SI-3)**. For the initial Pb^{2+} concentration of 300 µg/L in synthetic water at pH 7.8, 20 % and 47 % of $[Pb]_t$ were precipitated as $[Pb(OH)_2](s)$ and $[PbCO_3](s)$ respectively, however, in DI water, 93.7 % of $[Pb]_t$ was precipitated as $[Pb(OH)_2](s)$ and no $[PbCO_3](s)$ was formed.

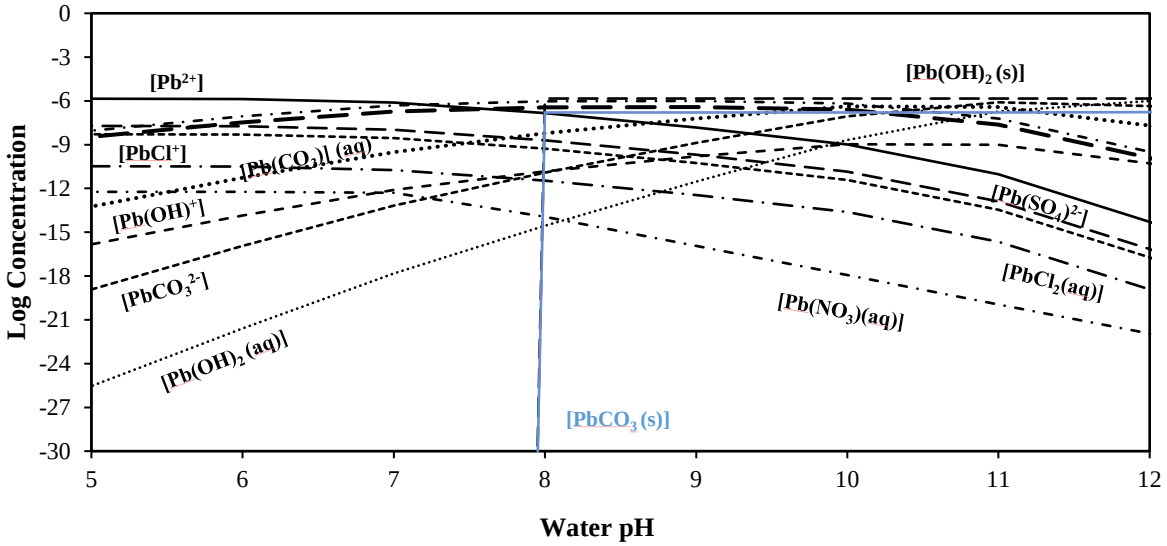

Figure 3: *Log concentrations for Pb^{2+} species versus the water pH, $[Pb]_t$ = 300 µg/L*

EFFECT OF ION'S COMPETITION ON Pb^{2+} DEPOSITION ONTO NEW AND AGED LDPE

Our results (**Figure 4**) demonstrated a significantly lower Pb^{2+} uptake by both new and aged LDPE pellets in synthetic drinking water compared to their Pb^{2+} uptake as reported by Salehi et al., (2018) in Ultrapure Millipore treated water under similar conditions (pH=7.8, $[Pb^{2+}]_t$=300 µg/L). This lower Pb uptake by LDPE pellets could be described in terms of the difference in the ionic strength of synthetic drinking water (0.0072 M) and DI water (3×10^{-6} M). Additional ions present in the synthetic water have competed with Pb species to occupy the LDPE available surface sites and resulted in the reduced Pb surface loading on LDPE pellets.[63] Surrounding the LDPE adsorption sites with counter ions present in synthetic water reduces their electrostatic attractions toward the Pb species existed in the aqueous environment.[64,65] Furthermore, the solutions great ionic strength reduces the activity coefficient of Pb^{2+} species, and limit their transfer to the LDPE surface.[66] The lower Pb^{2+} surface loading on new and aged LDPE pellets in synthetic water could be attributed to the competition of cations: K^+, Ca^{2+}, Na^+, Mg^{2+}, $Al^{3+,}$ and co-anions: Cl^-, SO_4^{2-}, HPO_4^{2-}, CO_3^{2-}, NO_3^- with Pb^{2+} for electrostatic binding to the LDPE surface.[67] Consequently, Pb^{2+} species adsorption become more competitive, in which different ions compete for a limited number of metal-binding sites on the LDPE surface. The degree of inhibition on Pb adsorption by available inorganic ions followed the sequence: $K^+ < Na^+ < Mg^{2+} < Ca^{2+} < Al^{3+}$. Na^+, K^+, $Mg^{2+}$and Ca^{2+} inhibited adsorption because they outcompeted Pb ions for adsorption sites this decreasing the activity of Pb ions.[68] As monovalent cations (Na^+ and K^+) are bound by ionic attraction, they do not compete directly with Pb ions to the binding sites onto the LDPE surface and therefore have less influence on the adsorption. Pb adsorption is influenced by the presence of anions following the order, $Cl^- > SO_4^{2-} > NO_3^-$.[67] The negative effect of Cl^-,

SO_4^{2-}, HPO_4^{2-} on Pb adsorption may be as a result of metal anion complexing since Pb^{2+} forms some soluble complexes with the anions.

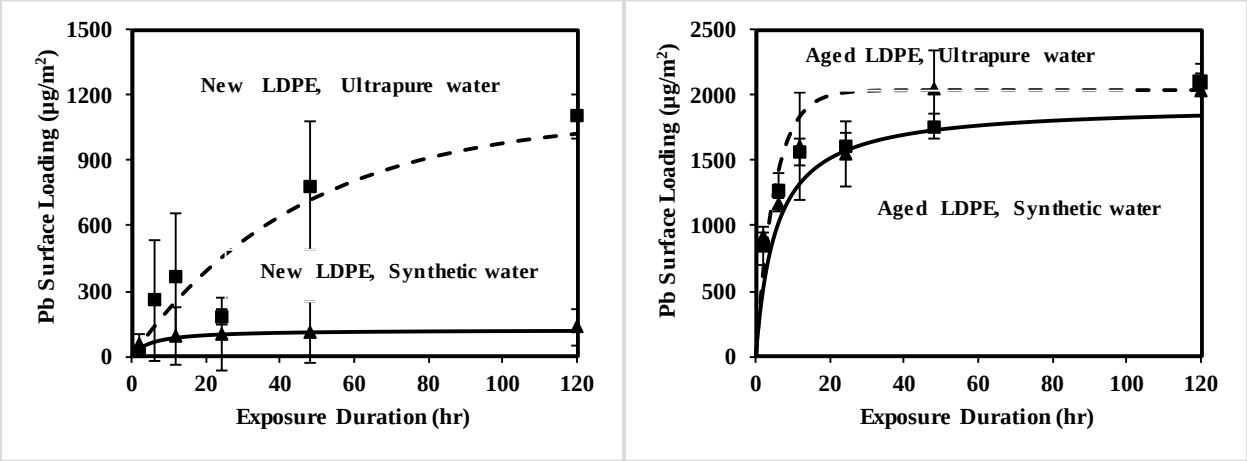

Figure 4: *Pb surface loading on (A) new LDPE and (B) aged LDPE in DI water and synthetic water at pH 7.8*

THE INFLUENCE OF CHLORINE RESIDUALS ON Pb DEPOSITION ONTO THE LDPE SURFACE

THE INFLUENCE OF CHLORINE RESIDUALS ON THE KINETICS OF Pb DEPOSITION ONTO NEW LDPE

The presence of chlorine residuals reduced Pb^{2+} adsorption onto the new LDPE surface during the entire exposure period (T_{stat} *= 11.50,* T_{crit} *= 2.57, p = 0.0003*). When no chlorine residual was present, the equilibrium Pb surface loading on LDPE pellets (135 µg/m^2) was significantly greater than the condition that chlorine residuals were present (95 µg/m^2). Both Pseudo 1st and 2nd order kinetic models were fitted into the experimental data to obtain a better understanding of chlorine residual impact on Pb adsorption mechanisms. The graphical demonstration of the Pseudo 1st order kinetic model and the kinetic rate constants are shown in **Table 2** and **Figure 5,** respectively. When there were no chlorine residuals in the system, LDPE

reached the equilibrium surface loading in a shorter time compared to the condition when the chlorine residuals were present. The chlorine decay has been investigated in the synthetic water containing LDPE pellets in the presence and absence of Pb^{2+}, using 1st order chlorine decay model during the five day exposure period.[69,70] No significant difference was found in the chlorine decay behavior due to the Pb presence in the aqueous solution (*p*-value>0.05). That might be due to the significantly lower concentration of Pb^{2+} (300 µg/L) compare to the total chlorine residuals (2 mg/L). Thus, the formation of possible chloro-complexes of Pb like, $PbCl^{+}$, $PbCl_2$, $PbCl_3^{-}$ and $PbCl_4^{2-}$ has not influenced the decay pattern. Negative correlation (-0.906) was found between Pb surface loading and total chlorine residual (*p*-value<0.05) suggesting the impact of chlorine residual in preventing the Pb species from adsorption onto the LDPE surface (**Figure SI-6**).

Table 2: *The influence of chlorine residuals on the kinetics of Pb adsorption onto new LDPE*

LDPE	Pseudo 1st order model			Pseudo 2nd order model			
	K (h^{-1})	R^2	$t_{½}$ (h)	$q_{eq,}$ Exp (µg/m^2)	K ($m^2µg^{-1}h^{-1}$)	R^2	$q_{eq,}$ Cal (µg/m^2)
No chlorine residuals	0.039	0.99	18	124.9	0.00040	0.97	135.4
With chlorine residuals	0.036	0.99	19.25	98.5	0.00085	0.99	119.1

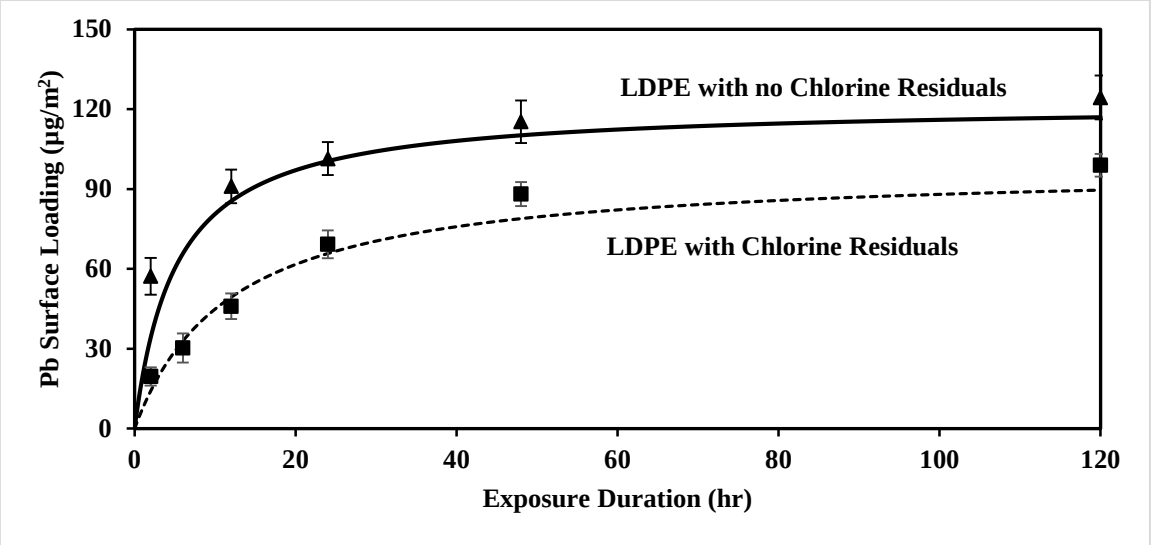

Figure 5*: Pb surface loading on LDPE with presence and absence of chlorine residuals*

OXIDATION OF LDPE SURFACE ACCUMULATED Pb^{2+} TO Pb^{4+}

Free chlorine residuals are capable of oxidizing Pb^{2+} to Pb^{4+} by forming PbO_2 precipitates in the aqueous solution and reduce the Pb accumulation onto the LDPE surface. [71] Additional XPS analysis was conducted to examine oxidation of LDPE surface accumulated Pb^{2+} to Pb^{4+} due to the exposure to chlorine residuals.

$$Pb^{2+} + HOCl + H_2O \rightarrow PbO_2 + HCl \qquad E_H^0 = 2.94\ (V) \qquad (10)$$

The additional XPS analysis was conducted to identify how exposure to the free chlorine residual alters the oxidation state of Pb ions deposited onto the LDPE surface. The Pb(4f) spectra for LDPE exposed to Pb only and Pb + free chlorine residuals are shown in **Figure 6**. The doublet peak of Pb 4f spectra for LDPE exposed to the Pb in absence of free chlorine residuals were located at 137.6 and 143 eV binding energies, respectively, and suggested the presence of Pb^{2+} in from of $Pb(OH)_2$ as predicted through precipitation reaction.[72] However, the shoulder peaks of Pb(4f) occurred in samples exposed to the free chlorine residuals. After decomposing its spectra through Gaussian-Lorentzian curve fitting, the binding energies of Pb(4f7/2 and 2f5/2) at 138.9

eV and 144.1 eV were associated with Pb^{4+}, and suggested oxidation of Pb^{2+} to Pb^{4+} through formation of PbO_2.[73,72] This curve fitting revealed that 58 % of total Pb deposited onto the LDPE surface was oxidized to Pb^{4+} due to the presence of free chlorine residual and the remaining 42 % was present as Pb^{2+}.

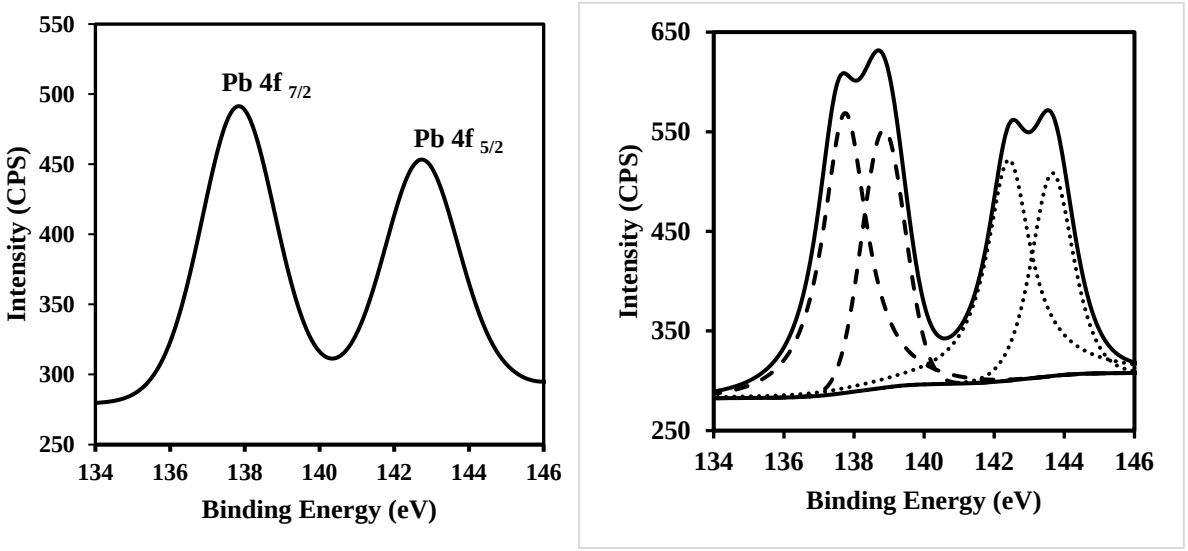

(A) 10 h aged LDPE + Pb **(B)** 10 h aged LDPE + Pb + Free chlorine residual

***Figure 6**: X-ray photoelectron spectroscopy (XPS) spectra of Pb*

INVESTIGATE THE FACTORS INFLUENCE Pb RELEASE FROM LDPE SURFACE

Pb release from LDPE surface into the synthetic water at pH 5.0 and 7.8 under dynamic condition during the 5-day release period is presented in (**Figure 7**). This suggests gradual detachment of Pb species accumulated onto the LDPE surface into the water, which might be due to the shear forces applied during the dynamic mixing along with the concentration gradient in the contact water. In response to the concentration gradient, diffusion of the Pb species from the LDPE surface into the contact water may occur and will continue until an equilibrium concentration is reached. The greatest level of Pb release into the contact water occurred by a

reduction of the pH of contact water from 7.8 to 5.0. After 5 min exposure to the synthetic water at pH 5.0, approximately 65 % of Pb^{2+} species were released however, only 4 % were released at pH 7.8. This could be due to the greater solubility of precipitated Pb^{2+} species at the lower pH levels.[74,75] The study conducted by Turner and Holmes (2015) also reported a lower level of Pb species left in the aqueous solution at pH 8.0 (~15 %) compared to the pH 5.0 (~30 %) after conducting the microplastics metal exposure experiment. [21] The literature investigated heavy metal release from plastic surface are limited. The recent study conducted by Fernández et al., (2020) demonstrated 37 % Hg released from virgin and non-aged micro plastics under dynamic flow condition in first 2 h contact with the sea water. This Hg release has been increased up to 12 % following 7 days exposure period. [76] However; in the present study, 73 % Pb was released after 2 h and approached to 86 % release after 5 days. Similar to our findings the metal species adsorbed onto immobile site of polymer surface have high stability constant which limits the rate of diffusion of Hg in the water. Moreover, as our speciation graph in **Figure 3** showed the primary forms of Pb^{2+} in water are $Pb(OH)_2$ and $PbCO_3$ precipitates (67 % of $[Pb]_t$) at pH 7.8, however by pH reduction to 5.0, these precipitates accumulated on LDPE surface could be dissolved into the water and be converted to the Pb^{2+} dissolved ions. At pH 5.0, a greater level of surface deposited Pb was released to the contact water under dynamic condition (86 % after 5 days) compared to the static condition (22 % after 5 days) (**Figure SI-7**).

The dynamic condition caused by stirring the LDPE pellets in synthetic water during the release experiments increased the percentage of Pb release, by accelerating the mass transfer of Pb out of the LDPE surface to the water.[77] Immobile water adjacent to the Pb accumulated LDPE surface was not well mixed with the bulk water; therefore, that declined the concentration gradient and might limit the Pb release under stagnant condition. The lower percentage of

surface accumulated Pb species was released from aged LDPE pellets (9 %) compared to the new LDPE pellets (65 %) after immediate exposure to synthetic water at pH 5.0 (**Figure 8**). This might be due to Pb species stronger surface attachments and electrostatic association to the oxidized LDPE surface.[19] This result agreed with Santos-Echeandía et al., (2020) findings which reported that highly degraded microplastics recovered from different beaches experienced a greater quantity of Hg deposition due to their anionic active surface sites and surface chemistry alterations caused by photooxidation. [22] Surprisingly, after a 24 h release period, instead of Pb releasing, some Pb species were absorbed onto the aged LDPE surface. This could be due to the electrostatic attraction of oxidized LDPE surface toward Pb species. However, initially, some of the adsorbed species were detached from the surface due to the concentration gradient and shear forces applied by stirring the solution, but they have resorbed onto the active surface sites over time.

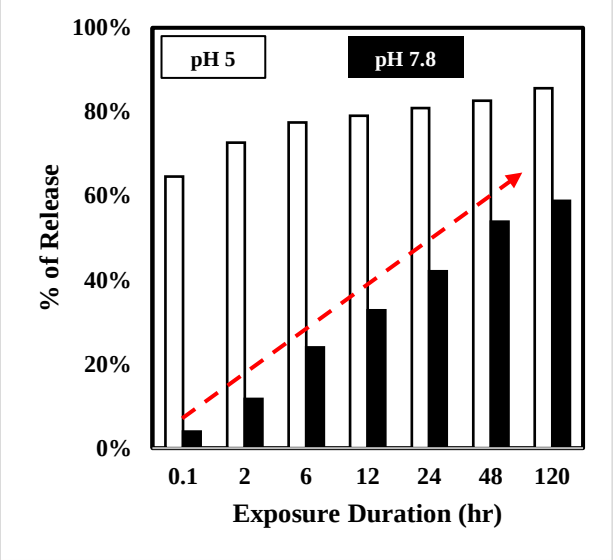

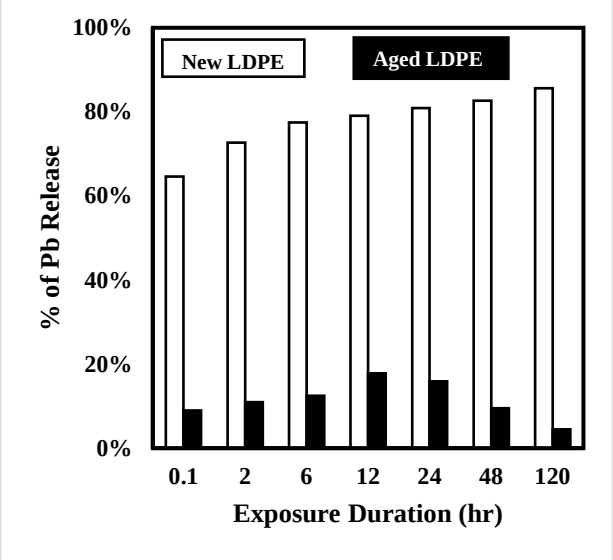

Figure 7: Percentage of Pb release from new LDPE at pH 5.0 and 7.8 (dynamic condition) (Left)

Figure 8: Percentage of Pb release from new and aged LDPE surface at pH 5.0 (dynamic condition) (Right)

IMPLICATION TO THE POTABLE WATER PLUMBING PIPES

Exposure to lead-contaminated tap water remains a serious public health concern nationally and globally. Plastic plumbing materials are increasingly being used to rehabilitate aging water infrastructure and construct new potable water systems as well as to limit cost and avoid drinking water quality and safety concerns associated with metal pipe corrosion. It is expected that replacing the corroded lead pipes with the plastic pipes will prevent lead exposure. However, other lead-bearing plumbing materials like brass valves and fittings, galvanized iron, lead-tin solders, and faucets could release lead into the water conveyed by the plastic plumbing. This study demonstrated that biofilm accumulation onto the plastic surface promotes the lead uptake. This finding along with the previous literature that indicated a greater biofilm accumulation onto the plastic plumbing than copper pipes raising concerns regarding an enhanced potential risk of plastic pipes toward the public safety compared to the copper pipes. [78,79,80] The variation of lead deposition onto and release from the plastic surface by water chemistry conditions highlights the role of water sources, treatment practices, and water quality fluctuations on lead mobility within the building plumbing systems. Furthermore, the greater number of available surface sites provided by the aged plastics for lead accumulation, underscores the importance of plastic pipes stability. This informs the plastic pipes' manufacturers to generate more thermo-oxidative resistance pipes to suppress the risk of lead accumulation within the plumbing while improving the pipes service life. This research revealed the significant role of chlorine residuals on reduced lead deposition onto the plastic pipes by forming the PbO_2(s) precipitates and inhibiting the biofilm development onto the pipe surface. Thus, the water distribution systems could reduce the degree of lead deposition onto the building plumbing by maintaining the proper level of disinfectant residuals. Lead deposition onto plastic pipes could become a public health threat, when these deposits are released into tap water. It was found that water chemistry fluctuations like pH reduction and chlorine concentration could result in Pb release from the plastic surface back to the drinking water. Thus, the water utilities using blending or differently source water

should develop strategies to avoid the significant water pH fluctuations within their network to limit the risk of metal release to the people's tap water. The Pb release pattern from the plastic surface could vary depending on the degree of plastic surface oxidation under static and dynamic conditions. These results are applicable in the new and aged polyethylene pipes used for the drinking water plumbing.

CONCLUSION

In this study, the influence of biofilm presence, water chemistry conditions, and chlorine residuals on Pb^{2+} deposition onto the LDPE surface was investigated. Two novel approaches have been developed to quantify the biofilm accumulated onto the LDPE surface and examine the interrelation between biofilm biomass and Pb^{2+} accumulation. In addition, the effect of water pH on Pb^{2+} release from LDPE surface was investigated under static and dynamic conditions. A more significant Pb surface loading was found on LDPE with biofilm (1602 $\mu g/m^2$) compare to LDPE with no biofilm (124 $\mu g/m^2$). The biofilm accumulation on the LDPE surface enhanced the surface sites available for Pb^{2+} adsorption and increased its uptake. The Pseudo 2nd order kinetic model was fitted into the experimental Pb^{2+} adsorption data for the LDPE surface with the biofilm. The greater ionic strength and competitive ions presence in aqueous solution significantly reduced Pb accumulation onto the LDPE surface. The presence of chlorine residuals in the aqueous solution resulted in the lower Pb uptake by the LDPE surface. The XPS spectroscopy confirmed oxidation of surface deposited Pb^{2+} to Pb^{4+} due to the exposure to free chlorine residuals. A higher level of Pb was released from the LDPE surface into the water under dynamic conditions compared to the static tests. A lower water pH increased the Pb release into the contact water under dynamic condition.

REFERENCES

1. Olson TM, Wax M, Yonts J, et al. Forensic estimates of lead release from lead service lines during the water crisis in Flint, Michigan. *Environ Sci Technol Lett*. 2017;4(9):356-361. doi:10.1021/acs.estlett.7b00226

2. Yang E, Faust KM. Dynamic public perceptions of water infrastructure in US shrinking cities: end-user trust in providers and views toward participatory processes. *J Water Resour Plan Manag*. 2019;145(9):1-13. doi:10.1061/(ASCE)WR.1943-5452.0001093

3. Edwards M, Triantafyllidou S, Best D. Elevated blood lead in young children due to lead-contaminated drinking water: Washington, DC, 2001-2004. *Environ Sci Technol*. 2009;43(5):1618-1623. doi:doi:10.1021/es802789w

4. Salehi M, Li X, Whelton AJ. Metal accumulation in representative plastic drinking water plumbing systems. *J Am Water Works Assoc*. 2017;109(11):E479-E493. doi:10.5942/jawwa.2017.109.0117

5. Jain NB, Laden F, Guller U, Shankar A, Kazani S, Garshick E. Relation between blood lead levels and childhood anemia in India. *Am J Epidemiol*. 2005;161(10):968-973. doi:10.1093/aje/kwi126

6. D. DeSimone, D. Sharafoddinzadeh MS. Prediction of children's blood lead levels from exposure to lead in schools' drinking water — A case study in Tennessee, USA. *Water Journal, Spec Issue Water Qual Build*. 2020;12(6). doi:doi.org/10.3390/w12061826

7. Boyd GR, Pierson GL, Kirmeyer GJ, English RJ. Lead variability testing in Seattle public schools. *J / Am Water Work Assoc*. 2008;100(2):53-64. doi:10.1002/j.1551-8833.2008.tb08142.x

8. Subramanian KS, Sastri VS, Elboujdaini M, Connor JW, Davey ABC. Water contamination: Impact of Tin-Lead solder. *Water Res*. 1995;29(8):1827-1836. doi:10.1016/0043-1354(95)00005-6

9. Salehi M, Odimayomi T, Ra K, et al. An investigation of spatial and temporal drinking water quality variation in green residential plumbing. *J Build Environ*. 2020;169(August 2019):106566. doi:10.1016/j.buildenv.2019.106566

10. Salehi M, Abouali M, Wang M, et al. Case study: Fixture water use and drinking water quality in a new residential green building. *Chemosphere*. 2018;195:80-89. doi:10.1016/J.CHEMOSPHERE.2017.11.070

11. Huang X, Zemlyanov DY, Diaz-Amaya S, Salehi M, Stanciu L, Whelton A. Competitive heavy metal adsorption onto new and aged polyethylene under various drinking water conditions. *J Hazard Mater*. 2019;385:127065. doi:10.1016/j.snb.2019.127065

12. Elfland C, Paolo S, Marc E. Lead-contaminated water from brass plumbing devices in new buildings. *J / Am Water Work Assoc*. 2010;102(11):66-76. doi:10.1002/j.1551-8833.2010.tb11340.x

13. Stewart BR. Corrosion resistance, ease of installation stimulate demand for plastic pipe. *Plast Eng*. 2005:14-22.

14. Rożej A, Cydzik-Kwiatkowska A, Kowalska B, Kowalski D. Structure and microbial diversity of biofilms on different pipe materials of a model drinking water distribution systems. *World J Microbiol Biotechnol*. 2015;31(1):37-47. doi:10.1007/s11274-014-1761-6

15. Shakhsi-Niaei M, Salehi Esfandarani M. Multi-objective deterministic and robust models for selecting optimal pipe materials in water distribution system planning under cost, health, and environmental perspectives. *J Clean Prod*. 2019;207:951-960. doi:10.1016/j.jclepro.2018.10.071

16. Whelton AJ, Nguyen T. Contaminant migration from polymeric pipes used in buried potable water distribution systems: A Review. *Crit Rev Environ Sci Technol*. 2013;43(7):679-751. doi:10.1080/10643389.2011.627005

17. LEED for homes rating system. *US Green Build Counc*. 2008.

18. Kelley KM, Stenson AC, Dey R, Whelton AJ. Release of drinking water contaminants and odor impacts caused by green building cross-linked polyethylene (PEX) plumbing systems. *Water Res*. 2014;67:19-32. doi:10.1016/j.watres.2014.08.051

19. Salehi M, Jafvert CT, Howarter JA, Whelton AJ. Investigation of the factors that influence lead accumulation onto polyethylene: Implication for potable water plumbing pipes. *J Hazard Mater*. 2018;347:242-251. doi:10.1016/j.jhazmat.2017.12.066

20. Holmes LA, Turner A, Thompson RC. Interactions between trace metals and plastic production pellets under estuarine conditions. *Mar Chem*. 2014;167:25-32. doi:10.1016/j.marchem.2014.06.001

21. Turner A, Holmes LA. Adsorption of trace metals by microplastic pellets in fresh water. *Environ Chem*. 2015;12(5):600-610. doi:10.1071/EN14143

22. Santos-Echeandía J, Rivera-Hernández JR, Rodrigues JP, Moltó V. Interaction of mercury with beached plastics with special attention to zonation, degradation status and polymer type. *Mar Chem*. 2020;222(October 2019):103788. doi:10.1016/j.marchem.2020.103788

23. Wang YIN, Xie Y, Li W, Wang Z, Giammar DE. Formation of lead (IV) oxides from lead (II) compounds. 2010;44(23):8950-8956. doi:10.1021/es102318z

24. Masters S, Welter GJ, Edwards M. Seasonal variations in lead release to potable water. *Environ Sci Technol*. 2016;50(10):5269-5277. doi:10.1021/acs.est.5b05060

25. Liu H, Korshin G V, Ferguson JF. Interactions of Pb (II)/Pb (IV) solid phases with chlorine and their effects on lead release. *Environ Sci Technol*. 2009;43(9):3278-3284. doi:10.1021/es803179b

26. Zhang Y, Edwards M. Effects of pH, chloride, bicarbonate, and phosphate on brass dezincification. *J Am Water Works Assoc*. 2011;103(4):90-102. doi:10.1002/j.1551-8833.2011.tb11438.x

27. Rajasekharan V V., Clark BN, Boonsalee S, Switzer JA. Electrochemistry of free chlorine and monochloramine and its relevance to the presence of Pb in drinking water. *Environ Sci Technol*. 2007;41(12):4252-4257. doi:10.1021/es062922t

28. Switzer JA, Rajasekharan V V., Boonsalee S, Kulp EA, Bohannan EW. Evidence that monochloramine disinfectant could lead to elevated Pb levels in drinking water. *Environ Sci Technol*. 2006;40(10):3384-3387. doi:10.1021/es052411r

29. Xie Y. Dissolution , formation , and transformation of the lead corrosion product PbO2 : Rates and mechanisms of reactions that control lead release in drinking water distribution systems. *Diss Washingt Univ Open Scholarsh*. 2010;(January).

30. González-Rivas F, Ripolles-Avila C, Fontecha-Umaña F, Ríos-Castillo AG, Rodríguez-Jerez JJ. Biofilms in the spotlight: detection, quantification, and removal methods. *Compr Rev Food Sci Food Saf*. 2018;17(5):1261-1276. doi:10.1111/1541-4337.12378

31. Beech IB, Sunner J. Biocorrosion: Towards understanding interactions between biofilms and metals. *Curr Opin Biotechnol*. 2004;15(3):181-186. doi:10.1016/j.copbio.2004.05.001

32. Niquette P, Servais P, Savoir R. Impacts of pipe materials on densities of fixed bacterial biomass in a drinking water distribution system. *Water Res*. 2000;34(6):1952-1956. doi:10.1016/S0043-1354(99)00307-3

33. Lehtola MJ, Laxander M, Miettinen IT, Hirvonen A, Vartiainen T, Martikainen PJ. The effects of changing water flow velocity on the formation of biofilms and water quality in pilot distribution system consisting of copper or polyethylene pipes. *Water Res*. 2006;40(11):2151-2160. doi:10.1016/j.watres.2006.04.010

34. Rummel CD, Jahnke A, Gorokhova E, Kühnel D, Schmitt-Jansen M. Impacts of biofilm formation on the fate and potential effects of microplastic in the aquatic environment. *Environ Sci Technol Lett*. 2017;4(7):258-267. doi:10.1021/acs.estlett.7b00164

35. Munier B, Bendell LI. Macro and micro plastics sorb and desorb metals and act as a point source of trace metals to coastal ecosystems. *PLoS One*. 2018;13(2):1-13. doi:10.1371/journal.pone.0191759

36. Rhoads WJ, Pruden A, Edwards MA. Interactive effects of corrosion, copper, and chloramines on legionella and mycobacteria in hot water plumbing. *Environ Sci Technol*. 2017;51(12):7065-7075. doi:10.1021/acs.est.6b05616

37. Vargas IT, Alsina MA, Pavissich JP, et al. Multi-technique approach to assess the effects of microbial biofilms involved in copper plumbing corrosion. *Bioelectrochemistry*. 2014;97:15-22. doi:10.1016/j.bioelechem.2013.11.005

38. Marsili E, Kjelleberg S, Rice SA. Mixed community biofilms and microbially influenced corrosion. 2018;(1982):2-7. doi:10.1080/154281196

39. Vasquez FA, Heaviside R, Tang Z, Taylor JS. Effect of free chlorine and chloramines on lead release in a distribution system. *J / Am Water Work Assoc*. 2006;98(2). doi:10.1017/CBO9781107415324.004

40. Peng CY, Hill AS, Friedman MJ, et al. Occurrence of trace inorganic contaminants in drinking water distribution systems. *J Am Water Works Assoc*. 2012;104(3):53-54. doi:10.5942/jawwa.2012.104.0042

41. Proctor CR, Rhoads WJ, Keane T, et al. Considerations for large building water quality

after extended stagnation. *AWWA Water Sci*. 2020;n/a(n/a):e1186. doi:10.1002/aws2.1186

42. Fish KE, Collins R, Green NH, et al. Characterisation of the physical composition and microbial community structure of biofilms within a model full-scale drinking water distribution system. *PLoS One*. 2015;10(2):1-22. doi:10.1371/journal.pone.0115824

43. Ohsumi T, Takenaka S, Wakamatsu R, et al. Residual structure of streptococcus mutans biofilm following complete disinfection favors secondary bacterial adhesion and biofilm re-development. *PLoS One*. 2015;10(1):1-12. doi:10.1371/journal.pone.0116647

44. Richter-Heitmann T, Eickhorst T, Knauth S, Friedrich MW, Schmidt H. Evaluation of strategies to separate root-associated microbial communities: A crucial choice in rhizobiome research. *Front Microbiol*. 2016;7(MAY):1-11. doi:10.3389/fmicb.2016.00773

45. Priester JH, Horst AM, Van De Werfhorst LC, Saleta JL, Mertes LAK, Holden PA. Enhanced visualization of microbial biofilms by staining and environmental scanning electron microscopy. *J Microbiol Methods*. 2007;68(3):577-587. doi:10.1016/j.mimet.2006.10.018

46. Huang X, Zemlyanov DY, Diaz-Amaya S, Salehi M, Stanciu L, Whelton AJ. Competitive heavy metal adsorption onto new and aged polyethylene under various drinking water conditions. *J Hazard Mater*. 2020;385:121585. doi:10.1016/j.jhazmat.2019.121585

47. Huang X, Zhao S, Abu-Omar M, Whelton AJ. In-situ cleaning of heavy metal contaminated plastic water pipes using a biomass derived ligand. *J Environ Chem Eng*. 2017;5(4):3622-3631. doi:10.1016/j.jece.2017.07.003

48. Huang X, Pieper KJ, Cooper HK, Diaz-Amaya S, Zemlyanov DY, Whelton AJ. Corrosion of upstream metal plumbing components impact downstream PEX pipe surface deposits and degradation. *Chemosphere*. 2019;236:124329. doi:10.1016/j.chemosphere.2019.07.060

49. Chen Z, Ma W, Han M. Biosorption of nickel and copper onto treated alga (undaria pinnatifida): Application of isotherm and kinetic models. *J Hazard Mater*. 2008;155(1-2):327-333. doi:10.1016/j.jhazmat.2007.11.064

50. Basha S, Murthy ZVP. Kinetic and equilibrium models for biosorption of Cr(VI) on chemically modified seaweed, cystoseira indica. *Process Biochem*. 2007;42(11):1521-1529. doi:10.1016/j.procbio.2007.08.004

51. Ho YS, McKay G. Pseudo-second order model for sorption processes. *Process Biochem*. 1999;34(5):451-465. doi:10.1016/S0032-9592(98)00112-5

52. Zhang C, Li C, Zheng X, Zhao J, He G, Zhang T. Effect of pipe materials on chlorine decay, trihalomethanes formation, and bacterial communities in pilot-scale water distribution systems. *Int J Environ Sci Technol*. 2017;14(1):85-94. doi:10.1007/s13762-016-1104-2

53. Lewandowski Z, Webb D, Hamilton M, Harkin G. Quantifying biofilm structure. *Water Sci Technol*. 1999;39(7):71-76. doi:10.1016/S0273-1223(99)00152-3

54. Yang X, Beyenal H, Harkin G, Lewandowski Z. Quantifying biofilm structure using image analysis. *J Microbiol Methods*. 2000;39(2):109-119. doi:10.1016/S0167-7012(99)00097-4

55. Salehi M, Johari MS. Study of fiber packing density of lyocell ring-spun yarns. *J Text Inst*. 2011;102(5):389-394. doi:10.1080/00405000.2010.482341

56. Yee N, Fein JB. Does metal adsorption onto bacterial surfaces inhibit or enhance aqueous metal transport? column and batch reactor experiments on Cd-bacillus subtilis-quartz systems. *Chem Geol*. 2002;185(3-4):303-319. doi:10.1016/S0009-2541(01)00412-0

57. Fein JB, Daughney CJ, Yee N, Davis TA. A chemical equilibrium model for metal adsorption onto bacterial surfaces. *Geochim Cosmochim Acta*. 1997;61(16):3319-3328. doi:10.1016/S0016-7037(97)00166-X

58. Muhammad N, Parr J, Smith MD, Wheatley AD. Microbial uptake of heavy metals in slow sand filters. *Environ Technol (United Kingdom)*. 1998;19(6):633-638. doi:10.1080/09593331908616720

59. Feder M, Phoenix V, Haig S, Sloan W, Dorea C, Haynes H. Influence of biofilms on heavy metal immobilization in sustainable urban drainage systems (SuDS). *Environ Technol (United Kingdom)*. 2015;36(21):2803-2814. doi:10.1080/09593330.2015.1049214

60. Suguna M, Siva Kumar N. Equilibrium, kinetic and thermodynamic studies on biosorption of lead(II) and cadmium(II) from aqueous solution by polypores biomass. *Indian J Chem Technol*. 2013;20(1):57-69.

61. Olu-Owolabi BI, Diagboya PN, Ebaddan WC. Mechanism of Pb2+ removal from aqueous solution using a nonliving moss biomass. *Chem Eng J*. 2012;195-196:270-275. doi:10.1016/j.cej.2012.05.004

62. Javanbakht V, Zilouei H, Karimi K. Lead biosorption by different morphologies of fungus mucor indicus. *Int Biodeterior Biodegrad*. 2011;65(2):294-300. doi:10.1016/j.ibiod.2010.11.015

63. Boudrahem F, Aissani-Benissad F, Soualah A. Adsorption of lead(II) from aqueous solution by using leaves of date trees as an adsorbent. *J Chem Eng Data*. 2011;56(5):1804-1812. doi:10.1021/je100770j

64. Vilar VJP, Botelho CMS, Boaventura RAR. Kinetics and equilibrium modelling of lead uptake by algae gelidium and algal waste from agar extraction industry. *J Hazard Mater*. 2007;143(1-2):396-408. doi:10.1016/j.jhazmat.2006.09.046

65. Unuabonah EI, Adebowale KO, Olu-Owolabi BI, Yang LZ, Kong LX. Adsorption of Pb (II) and Cd (II) from aqueous solutions onto sodium tetraborate-modified kaolinite clay: equilibrium and thermodynamic studies. *Hydrometallurgy*. 2008;93(1-2):1-9. doi:10.1016/j.hydromet.2008.02.009

66. Wu XL, Zhao D, Yang ST. Impact of solution chemistry conditions on the sorption behavior of Cu(II) on Lin'an montmorillonite. *Desalination*. 2011;269(1-3):84-91. doi:10.1016/j.desal.2010.10.046

67. Inglezakis VJ, Zorpas AA, Loizidou MD, Grigoropoulou HP. The Effect of competitive cations and anions on ion exchange of heavy metals. *Sep Purif Technol*. 2005;46(3):202-207. doi:10.1016/j.seppur.2005.05.008

68. Liu W, Wang T, Borthwick AGL, et al. Adsorption of Pb2+ , Cd2+ , Cu2+ and Cr3+ onto titanate nanotubes: Competition and effect of inorganic ions. *Sci Total Environ*. 2013;456-457:171-180. doi:10.1016/j.scitotenv.2013.03.082

69. Powell BJC, West JR, Hallam NB, Forster CF. Performance of various kinetic models for chlorine decay. *Water Resour*. 2000;126(February):13-20. doi:10.1061/(ASCE)0733-9496(2000)126:1(13)

70. Powell JC, Hallam NB, West JR, Forster CF, Simms J. Factors which control bulk chlorine decay rates. *Water Res*. 2000;34(1):117-126. doi:10.1016/S0043-1354(99)00097-4

71. Zhang Y, Lin YP. Determination of PbO2 formation kinetics from the chlorination of Pb(II) carbonate solids via direct PbO2 measurement. *Environ Sci Technol*. 2011;45(6):2338-2344. doi:10.1021/es1039826

72. Pederson LR. Two-dimensional chemical-state plot for lead using XPS. *J Electron Spectros Relat Phenomena*. 1982;28(2):203-209. doi:10.1016/0368-2048(82)85043-3

73. Murray JW. X-Ray photoelectron spectroscopic (XPS) studies on the chemical nature of metal ions adsorbed on clays and minerals. *Adsorpt From Aqueous Solut*. 1981;(January). doi:10.1007/978-1-4613-3264-0

74. Kim EJ, Herrera JE, Huggins D, Braam J, Koshowski S. Effect of pH on the concentrations of lead and trace contaminants in drinking water: A combined batch, pipe loop and sentinel home study. *Water Res*. 2011;45(9):2763-2774. doi:10.1016/j.watres.2011.02.023

75. Lasheen MR, Sharaby CM, El-Kholy NG, Elsherif IY, El-Wakeel ST. Factors influencing lead and iron release from some egyptian drinking water pipes. *J Hazard Mater*. 2008;160(2-3):675-680. doi:10.1016/j.jhazmat.2008.03.040

76. Fernández B, Santos-Echeandía J, Rivera-Hernández JR, Garrido S, Albentosa M. Mercury interactions with algal and plastic microparticles: Comparative role as vectors of metals for the mussel, Mytilus galloprovincialis. *J Hazard Mater*. 2020;396:122739. doi:10.1016/j.jhazmat.2020.122739

77. Xie Y, Giammar DE. Effects of flow and water chemistry on lead release rates from pipe scales. *Water Res*. 2011;45(19):6525-6534. doi:10.1016/j.watres.2011.09.050

78. Lehtola MJ, Miettinen IT, Keinänen MM, et al. Microbiology, chemistry and biofilm development in a pilot drinking water distribution system with copper and plastic pipes. *Water Res*. 2004;38(17):3769-3779. doi:10.1016/j.watres.2004.06.024

79. Taylor P, Percival SL, Walker JT. Biofouling : The journal of bioadhesion and biofilm Potable water and biofilms : A review of the public health implications potable water and biofilms : A review of the public health implications. 2009;(May 2014):37-41. doi:10.1080/08927019909378402

80. Liu G, Tao Y, Zhang Y, et al. Hotspots for selected metal elements and microbes accumulation and the corresponding water quality deterioration potential in an unchlorinated drinking water distribution system. *Water Res*. 2017;124:435-445. doi:10.1016/j.watres.2017.08.002

SUPPLEMENTAL INFORMATION

SI-1 MATERIALS

The LDPE films were used for XPS analysis, biofilm growth and quantification experiments. LDPE pellets were used for all other experiments. As reported by the company, the Pb ICP-MS standard was produced by dissolving Pb metal in HNO^3. Rhodamine 6G (C28-H31-N2-O3.Cl) stain is brownish-red in color, solid (powder) and chemically stable. Phosphate-buffered saline (PBS) was used for washing cells before dissociation, diluting cells for counting, and preparing reagents. It should be noted that different forms of LDPE used in this study may differ a little in their chemical compositions.

SI-2 CONDITIONING THE NEW AND AGED LDPE PELLETS

For conditioning, 15 g of pellets were initially rinsed three times with water; then they were stirred with 250 mL water for 24 h, then rinsed three times again with water, and finally dried at room temperature.

SI-3 CONTROL EXPERIMENT FOR MICROBIAL CELL SEPARATION METHOD VALIDATION

After taking out the LDPE films from the biofilm growing system, the films were stained with 5 µL of rhodamine 6G for 3 min and rinsed with a PBS buffer solution. Fluorescent images were taken on nine squares (16 mm × 16 mm) for each film (before separation). These films were placed in a 15 mL centrifuge tube containing 3 mL of PBS buffer solution (2X) on a shaker for 15 mins. After that, washed films were sonicated using a sonication probe for 5 mins. These sonicated films were stained with 5 µL of rhodamine 6G for 3 mins and rinsed with a PBS buffer solution and took the fluorescent images (after separation).

SI-4 XPS ANALYSIS

The X-ray power of 75 W at 12 kV was used for all experiments with a spot size of 400 μm^2. The base pressure of the K-Alpha instrument was at 1.0 x 10-9 mBa. The instrument was calibrated using Au 4f7/2 at 84.0 eV and Cu 2p3/2 at 932.67 eV. The C 1s line of 284.6 eV binding energy of absorbed hydrocarbon layer was used for spectra calibration. The XPS data acquisition was performed using the "Avantage v5.995" software provided with the instrument. Curve-fitting was performed after the base line was subtracted. The peak fitting procedure was repeated until a good fit was obtained.

Table SI-1: The chemical composition of synthetic tap water

Chemical Compounds	**Concentration (g/L)**
$MgSO_4.7H_2O$	0.2008
$Al_2(SO_4)_3.18H_2O$	0.0037
KNO_3	0.0127
$NaHCO_3$	0.0392
$Na_2SiO_3.9H_20$	0.0493
$CaSO_4.2H_2O$	0.0506
$CaCl_2.2H_2O$	0.0286
$Na_2HPO_4.7H_2O$	0.0001

Table SI-2: The chemical characteristics of the municipal tap water

	Parameter (Unit of Measure)	**Average Level Detected**
Water Quality Parameters	Alkalinity (mg/L)	52
	Calcium (mg/L)	9.5
	Chloride (mg/L)	5.3
	Hardness (mg/L)	45
	Hardness (mg/L as $CaCO_3$)	2.7

Inorganic Materials	Iron (mg/L)	0.03
	pH (Standard)	7.2
	Phosphate (mg/L)	1.03
	Sulfate (mg/L)	22.2
	Temperature (°F)	65.1
	Fluoride (mg/L)	0.6
	Nitrate as Nitrogen (N) (ppm)	0.06
	Sodium (mg/L)	8.63
	Lead (mg/L)	8.72
	Copper (mg/L)	0.30
Disinfection By-products	Total Trihalomethanes (mg/L)	BDL - 17.0
	Haloacetic Acids (HAA5) (mg/L)	BDL - 4.9
	Chlorine (mg/L)	1.05 - 1.5

Table SI-3: The chemical equilibrium and constants used to determine Pb speciation in synthetic water

Chemical Equilibrium	**Equilibrium Constant**
$Pb^{2+} + H_2O \rightleftharpoons PbOH^+ + H^+$	$\log\beta_1^* = -7.597$
$Pb^{2+} + 2H_2O \rightleftharpoons Pb(OH)_2^0 + 2H^+$	$\log\beta_2^* = -19.988$
$Pb^{2+} + 3H_2O \rightleftharpoons Pb(OH)_3^- + 3H^+$	$\log\beta_3^* = -28.091$
$Pb^{2+} + 4H_2O \rightleftharpoons Pb(OH)_4^{2-} + 4H^+$	$\log\beta_4^* = -39.699$
$Pb(OH)_2(S) + 2H^+ \rightleftharpoons Pb^{2+} + 2H_2O$	$K_s^* = 8.15$
$Pb^{2+} + CO_3^{2-} \rightleftharpoons Pb(CO_3^0)$	$\log\beta_1^* = 6.478$
$Pb^{2+} + 2CO_3^{2-} \rightleftharpoons Pb(CO_3)_2^{2-}$	$\log\beta_1^* = 9.938$
$Pb^{2+} + 2SO_4^{2-} \rightleftharpoons Pb(SO_4)_4^{2-}$	$\log\beta_1^* = 3.47$

$Pb^{2+} + Cl^{-} \leftrightarrow PbCl^{+}$	$\log\beta_1^* = 1.55$
$Pb^{2+} + 2Cl^{-} \leftrightarrow PbCl_2$	$\log\beta_1^* = -2.20$
$Pb^{2+} + NO_3^- \rightleftharpoons Pb(NO_3^+)$	$\log\beta_1^* = 1.17$

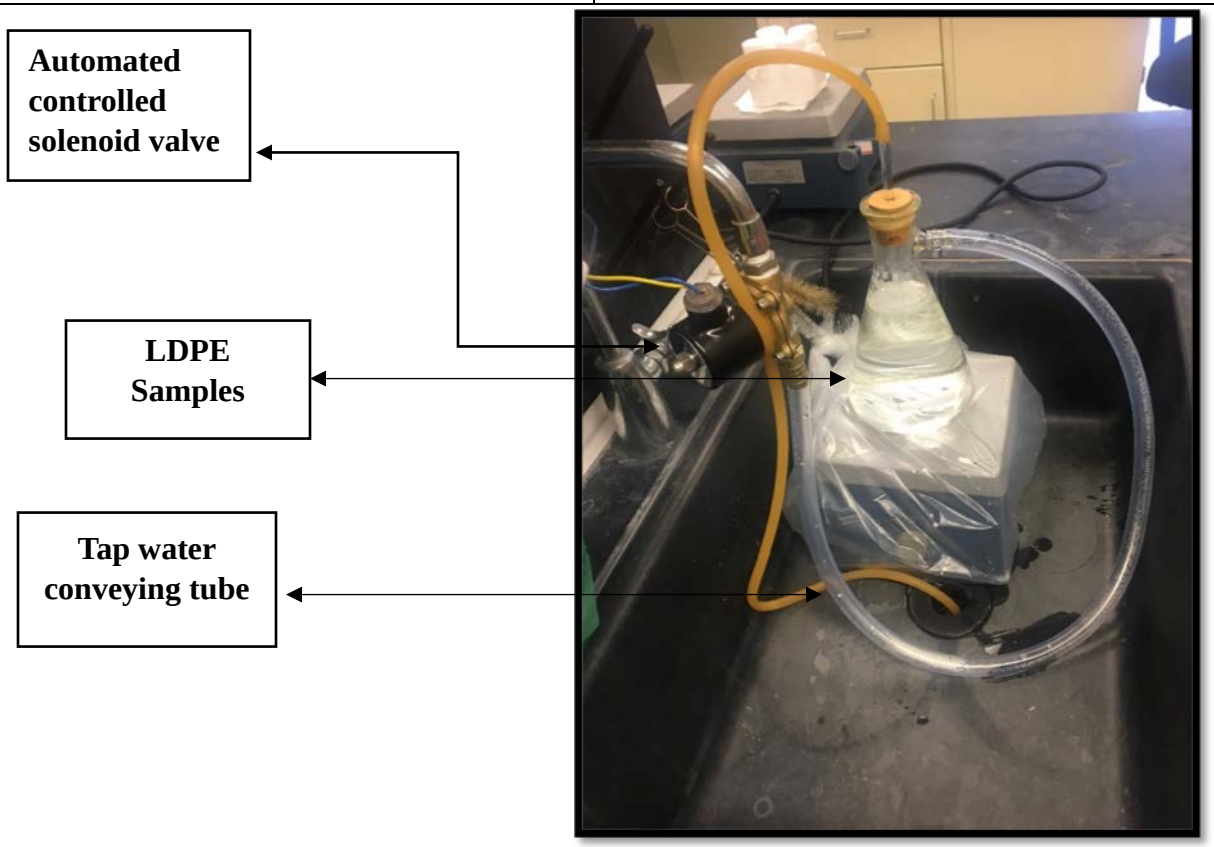

Figure SI-1: Biofilm development onto LDPE surface system setup

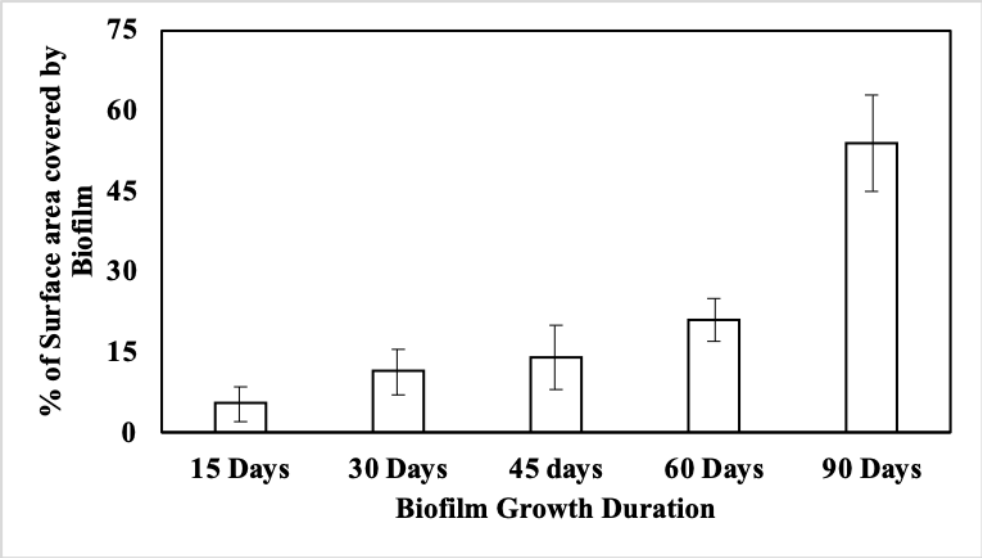

Figure SI-2: Percentage of surface area of LDPE film covered by biofilm over the time

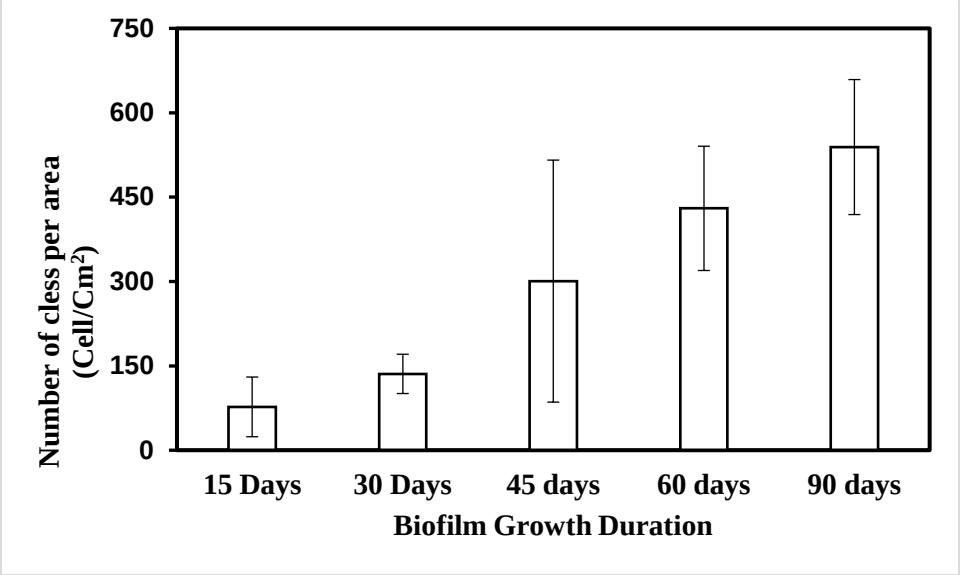

Figure SI-3: Number of cells per unit area of LDPE film during the biofilm growth period

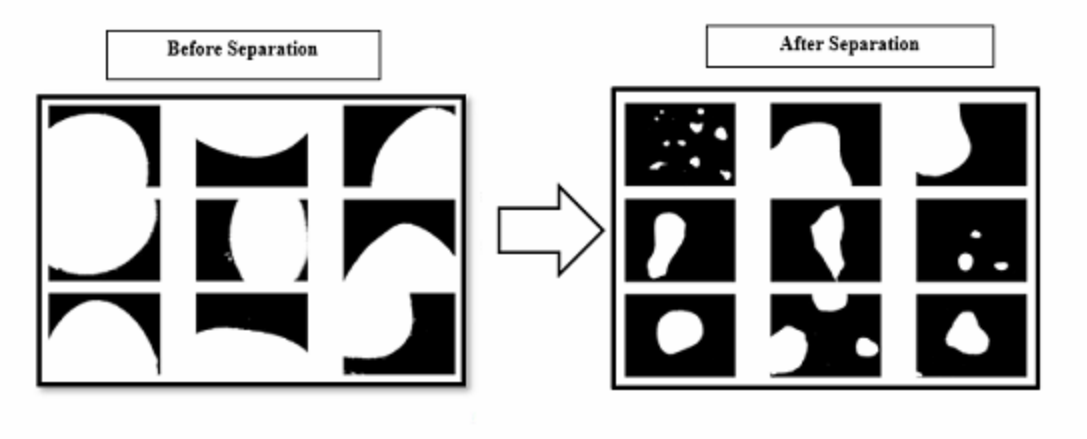

Figure SI-4: Control experiment for microbial cell separation method validation

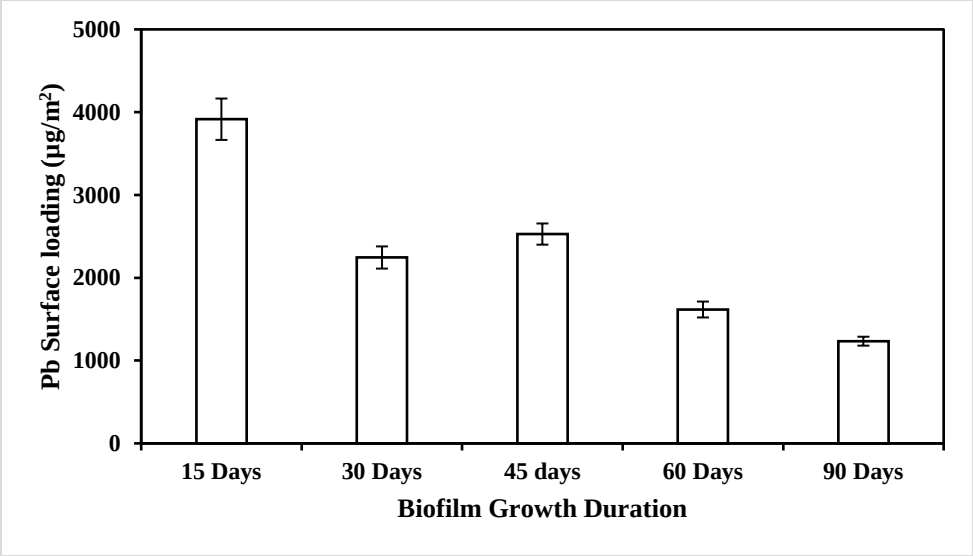

Figure SI-5: Pb deposition onto LDPE surface at different microbial growing duration

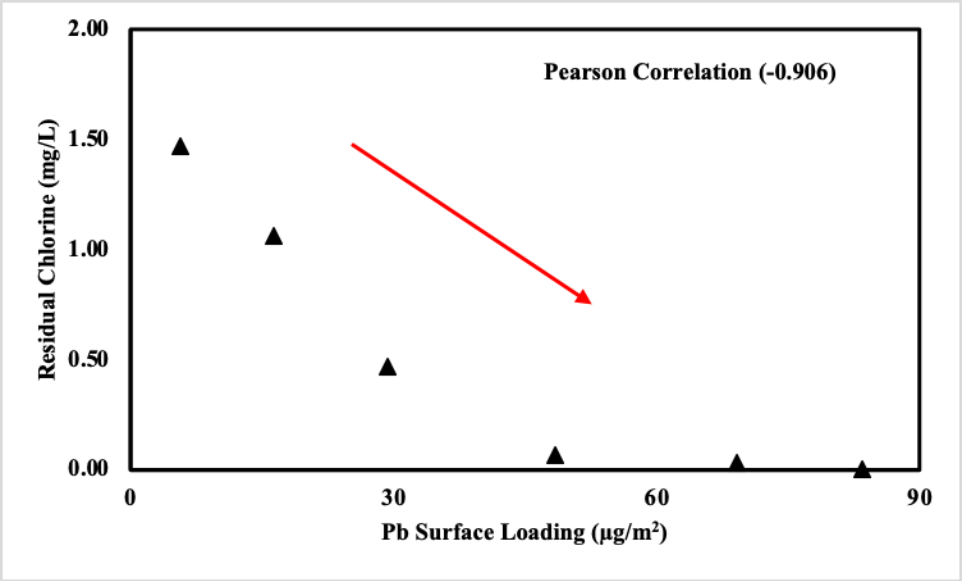

Figure SI-6: Correlation between Pb surface loading and residual chlorine

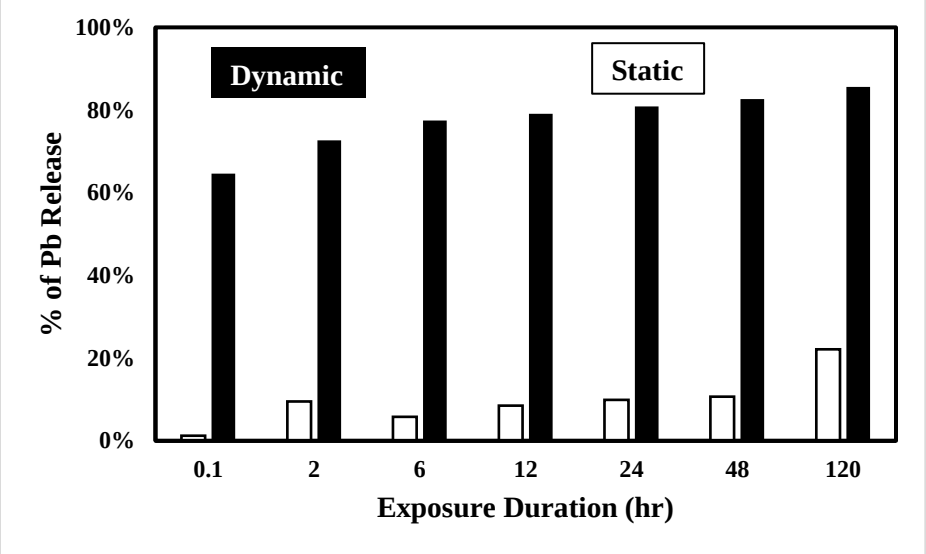

Figure SI-7: Percentage of Pb release from new LDPE surface at pH 5.0